Magnetic Resonance in Medicine 41:676–685 (1999)

In Vivo Observation of Lactate Methyl Proton Magnetization Transfer in Rat C6 Glioma

Yanping Luo,[1] Jan Rydzewski,[2] Robin A. de Graaf,[1] Rolf Gruetter,[1] Michael Garwood,[1] and Thomas Schleich[2]*

Magnetic resonance spectroscopy (MRS) measurements of the lactate methyl proton in rat brain C6 glioma tissue acquired in the presence of an off-resonance irradiation field, analyzed using coupled Bloch equation formalism assuming two spin pools, demonstrated the occurrence of magnetization transfer. Quantitative analysis revealed that a very small fraction of lactate ($f = 0.0012$) is rotationally immobilized despite a large magnetization transfer effect. Off-resonance rotating frame spin-lattice relaxation studies demonstrated that deuterated lactate binds to bovine serum albumin and the proteins present in human plasma, thereby providing a possible physical basis for the observed magnetization transfer effect. These results demonstrate that partial or complete saturation of the motionally restricted lactate pool (as well as other metabolites) by the application of an off-resonance irradiation field, such as that used for water presaturation, can lead to a substantial decrease in resonance intensity by way of magnetization transfer effects, resulting in quantitation errors. Magn Reson Med 41:676–685, 1999.

Key words: magnetization transfer; MRS visibility; rotational diffusion; rotational correlation time; lactate; glioma

Prominent among the proton resonances detected by in vivo magnetic resonance spectroscopy (MRS) are those of lactate, a metabolite indicative of brain pathology. Measurement of lactate tissue levels have potential for the evaluation of tumor malignancy (1–5) and brain ischemia (6,7), whereas lactate turnover measurements have been used for the assessment of metabolic activity (8,9). Reliable interpretation of MRS-derived metabolic measurements requires knowledge of the factors affecting lactate resonance intensity.

Proper quantification of metabolite magnetic resonance intensities necessitates that spin-lattice (T_1) and transverse (T_2) relaxation times be known. Even when relaxation effects are carefully taken into consideration, in vivo metabolite concentrations measured by MRS may still not reflect the actual concentration if the metabolite is engaged in binding to slowly tumbling tissue macromolecular species, thus rendering MRS invisible because of shortened relaxation times. Hence, under this circumstance it is possible that not all molecules of a given metabolite present in tissue contribute fully to the observed MRS signal. Recently, the MRS visibility of some commonly observed metabolites [choline, creatine, and N-acetyl aspartate (NAA)] was evaluated. Creatine in rat brain was found to be partially MRS invisible (10), whereas studies on brain cells (11) and postmortem rat brain (12,13) revealed a deficit in lactate concentration when measured by MRS relative to the values obtained by biochemical techniques. These observations suggested that a fraction of the lactate signal was MRS invisible, thereby introducing complications into the quantitative interpretation of the lactate proton resonance intensity.

The MRS visibility of a metabolite is strongly dependent on rotational mobility. A molecule freely tumbling in solution will have a relatively long T_2 relaxation time because intermolecular dipole-dipole interactions contributing to relaxation are largely averaged out, whereas molecules that are motionally restricted (e.g., by binding to macromolecules), by contrast, will experience net dipole interactions, and thus have a relatively short T_2 relaxation time, leading to a broader, potentially unobservable MRS signal.

Magnetization transfer (14,15) and off-resonance rotating frame spin-lattice relaxation experiments (16,17) are examples of off-resonance irradiation MRS experiments that provide a means for establishing the presence of motionally restricted metabolites. In this work, we used off-resonance irradiation MRS experiments to examine the in vivo occurrence of motionally restricted (and hence potentially MRS invisible) lactate, in brain tumor tissue. MRS spectral data for the lactate methyl proton in C6 glioma tissue acquired in the presence of off-resonance irradiation were analyzed using Bloch equations incorporating magnetization transfer (15) and off-resonance rotating frame spin-lattice relaxation formalism (16). Further interpretation was accomplished using the results of model lactate rotational diffusion studies performed in the presence of bovine serum albumin (BSA), and the proteins present in human plasma, by off-resonance rotating frame spin-lattice relaxation (16), a technique sensitive to the rotational dynamics of bound ligand molecules (17).

THEORY

We assume that tissue lactate is composed of two components, exhibiting liquid (mobile) and solid-like relaxation behavior (motionally restricted), respectively. The relaxation of the mobile metabolite protons is coupled, by way of chemical exchange or through-space dipolar interactions, to that of the less mobile (i.e., motionally restricted) metabolite protons. Because of magnetization exchange or transfer (cross-relaxation) between the two metabolite pools,

[1]Center for Magnetic Resonance Research and Clinical Research Center, Department of Radiology, University of Minnesota, Minneapolis, Minnesota.

[2]Department of Chemistry and Biochemistry, University of California, Santa Cruz, California.

Grant sponsor: National Institutes of Health; Grant numbers: EY-04033 and CA-64338.

A preliminary account of this work was presented at the Third Scientific Meeting and Exhibition of the Society of Magnetic Resonance, Nice, France, 1995.

*Correspondence to: Thomas Schleich, Department of Chemistry and Biochemistry, University of California, Santa Cruz, CA 95064.

Received 3 June 1998; revised 18 September 1998; accepted 30 September 1998.

alterations in the nuclear spin relaxation of one pool will affect the relaxation in the other.

Magnetization transfer between protein protons and solvent-water protons, mediated by cross-relaxation, has been exploited by Wolff and Balaban (14) in off-resonance irradiation experiments and is commonly used to enhance contrast in MRI. The essence and theory of the off-resonance irradiation experiment for the study of rotational diffusion has been described in detail by Schleich et al (16).

Bloch Equation Formalism

The steady-state solution of the Bloch equations incorporating magnetization transfer arising from off-resonance irradiation for an assumed two spin-component system is given elsewhere (15,18).

The relevant parameters of the steady-state solution of the Bloch equations defining magnetization transfer are as follows: $R_{A,B}$ are the rate constants for spin-lattice relaxation of the A and B spins, respectively, in the *absence* of cross relaxation where the subscripts A and B denotes the mobile and motionally restricted spin pools, respectively; R_T is the cross-relaxation rate constant for magnetization transfer from the A to the B spin system. By contrast, R_T/f represents the rate constant for magnetization transfer from B to A, where $f\,(= M_o^B/M_o^A)$ is the ratio of the B spins to the number of A spins. We assumed that the frequency offsets $\nu_{off,A} = \nu_{off,B}$ and the preparation radiofrequency (RF) irradiation field strengths of the A and B spins, $B_{2A,B}$, respectively, were equal.

The steady-state solution of the Bloch equations incorporating magnetization transfer is equal to the steady-state solution derived by using the formalism of off-resonance rotating-frame spin-lattice relaxation (15).

The spin-lattice relaxation rates of the A and B spins in the *absence* of cross relaxation *cannot* be measured directly in coupled systems because of cross-relaxation contributions. Solution of the pair of coupled longitudinal relaxation equations assuming the absence of off-resonance irradiation on spin pool B, a small B spin pool size relative to the A pool ($f < 0.3$), and steady-state exchange between the two spin pools (i.e., $dM_z^B/dt = 0$), yields an expression describing the effect of exchange on the observed spin-lattice relaxation rate of the A (mobile) spin pool (14,19,20):

$$R_A = R_A^{obs} - \frac{R_T}{1 + \dfrac{R_T}{fR_B}} \qquad [1]$$

from which the intrinsic relaxation rate R_A can be indirectly determined using the observed relaxation times and relevant magnetization transfer parameters.

Assuming the absence of off-resonance irradiation on spin pool B, a small B spin pool size relative to the A pool, and $R_T/f \gg (R_B - R_{A,obs})$, a more general solution can be obtained by solving the pair of coupled longitudinal relaxation equations (21).

Adopting the assumptions described above for the spin-lattice relaxation time, a somewhat different derivation yields an analogous expression to Eq. [1] for T_2, assuming fast exchange, and a negligible difference in chemical shift for the A and B spins (19). Because the motionally restricted spin pool invariably has a very short T_2 relaxation time, typically on the order of 10 μsec, the contribution of T_2 relaxation from this spin pool can be ignored when R_T/f, the rate constant for magnetization transfer from the motionally restricted to the mobile spin pool, is small ($<10^4$). Eq. [1] becomes:

$$T_{2A} = \frac{T_{2A}^{obs}}{1 - R_T T_{2A}^{obs}}. \qquad [2]$$

Replacing the intrinsic relaxation parameters R_A and T_{2A} in the steady-state solution of the Bloch equations incorporating magnetization transfer with Eqs. [1] and [2], respectively, allows a four-parameter fit to be performed on the intensity ratio dispersion curve to obtain quantitative information about R_T, f, R_B, and T_{2B}.

Off-Resonance Rotating Frame Spin-Lattice Relaxation Considerations

Off-resonance irradiation may also give rise to off-resonance rotating frame spin-lattice relaxation effects in the absence of chemical exchange that are manifested by a reduction in resonance signal intensity. Under saturating conditions ($T_1T_2(\gamma B_2)^2 \gg 1$) and when the frequency offset $|\nu_{off}| \gg 1/T_2$ the relative magnetization (intensity ratio) can be expressed by the following equation (14,16,22,23):

$$\left(\frac{M_z}{M_o}\right)_{off\text{-}reson} = \left[1 + \frac{T_1}{T_2}\left(\frac{\gamma_H B_2}{\nu_{off}}\right)^2\right]^{-1}, \qquad [3]$$

thus providing a particularly straightforward expression for evaluating the occurrence of off-resonance rotating frame spin-lattice relaxation effects. This equation is identical to the Bloch expression for z-magnetization.

Equation [3] is useful for ascertaining the presence of magnetization transfer effects, for determining the percentage saturation of a spin pool at a given frequency offset (ν_{off}) and B_2 field strength ($\gamma_H B_2$), when T_1 and T_2 are known.

^{2}H Rotating Frame Spin-Lattice Relaxation

The ^{2}H off-resonance rotating frame spin-lattice relaxation experiment involves measurement of the resonance signal intensity after the application of a continuous-wave low-power RF irradiation field at a frequency off-resonance from the resonance(s) of interest for a time approximately equal to 5 T_1. The spectral intensity ratio ($R = M_z/M_o$) is equal to $\cos^2\Theta[T_{1\rho}^{off}/T_1]$, where Θ is the angle between the effective field (B_{eff}) and the z-axis, and $T_{1\rho}^{off}$ and T_1 are the spin-lattice magnetic relaxation times of the nuclear spins in the presence and absence of the RF field, respectively. The angle Θ is dependent on both B_2 and the frequency offset (ν_{off}) of the RF irradiation field. The theoretical expression for the relaxation rate constant describing spin relaxation along the effective field, $1/T_{1\rho}^{off}$, of a quadrupolar nucleus ($I = 1$), assuming axial symmetry for the electric field tensor, appears elsewhere (24). Theoretical expressions for ^{2}H T_1 and T_2 relaxation times, assuming a

dominant quadrupolar relaxation mechanism, are also given elsewhere (24).

Computer Simulations of Ligand Isotropic Reorientational Motion

Computer simulations have demonstrated the dependence of the ^2H spectral intensity ratio dispersion curves (R vs. ν_{off}) at constant B_2 field strength) on the fraction of bound ligand (χ_B), and the isotropic rotational correlation times of the bound ($\tau_{o,B}$) and free ($\tau_{o,F}$) ligand species (17). These simulations demonstrate the sensitivity of the intensity ratio dispersion curves to the fraction of bound ligand at fraction-bound values of less than 0.14 ($\tau_{o,F}$ = 0.01 nsec), whereas at fraction-bound values above 0.2, little or no change in dispersion curve behavior was observed.

MATERIALS AND METHODS

Tumor Induction and Animal Maintenance

C6 glioma cells (American Type Culture Collection, Rockville, MD) were cultured in Eagle's minimal essential medium (MEME; Celex, St. Louis, MO) containing 10% fetal bovine serum (Sigma, St. Louis, MO) and 1% penicillin-streptomycin antibiotics (Gibco BRL, Life Technologies, Grand Island, NY) under an atmosphere of 5% CO_2. Monolayer cells were trypsinized using 0.25% trypsin-EDTA (Gibco BRL, Life Technologies), harvested, and suspended in MEME at a concentration of 10^5 cells/mL.

Male Fisher rats (F344) (Harlan/Sprague-Dawley, Indianapolis, IN), weighing 225–250 g, were anesthetized by intramuscular injection (0.5 mL/250 g body weight) of a mixture composed of 1:1:4:1 of acepromazine (10 mg/mL; Ayerst, New York, NY), xylazine (20 mg/mL, Phoenix, St. Joseph, MO), ketamine (100 mg/mL, Ketlar; ParkDavis, Morris Plains, NJ), and saline. A stereotactic device was used to maintain rat brain position. An incision was made in the skin of the rat head through which a burr hole situated 2 mm laterally and 2 mm posterior was drilled into the bregma of the right hemisphere in the cortical region, followed by injection of 10 μL of C6 glioma cell suspension. The burr hole was sealed with bone-wax (Lukens, Lynchburg, VA) and the skin closed with skin clips.

Tumors were allowed to grow for 15–17 days to a size of 150–300 μL. Animals were anesthetized and then intubated. Long-duration anesthesia was maintained by ventilating the animals with a 1:1 gas mixture of N_2O and O_2 containing 1% isoforane (Ohmeda PPD, Liberty Corner, NJ). Capnography was performed to ensure proper ventilation throughout the experiment. Body temperature was maintained at 37°C using a warm water circulation system.

Proton MRS Experiments

All in vivo MRS measurements were performed on an Oxford 4.7 T 40 cm bore magnet interfaced to a Varian spectrometer console. A 15 mm diameter surface coil was used for both RF transmission and signal detection. A spherical phantom containing aqueous lactate (15 mM in saline) was used as a reference for the assessment of magnetization transfer.

T_2-weighted scout images were acquired using an adiabatic spin-echo sequence to determine appropriate localization for ^1H spectroscopy. Fig. 1 shows a typical coronal scout image with the ^1H MRS voxel used. The sequence used for ^1H MRS (Fig. 2) combines iOVS-ISIS for 3D localization (25) and gradient-enhanced multiple quantum coherence (geMQC) for lactate editing (26,27). We have previously shown that this geMQC editing sequence suppresses mobile lipid signals below detection (26). Prior to the application of the main pulse sequence, an off-resonance RF rectangular pulse of field strength 0.08–0.15 Gauss ($\gamma B_2/2\pi$ = 350–625 Hz) was applied for 3 sec at different frequency offsets varying from −100 kHz to +100 kHz with respect to the lactate methyl resonance at 1.3 ppm. A total of 33–40 points was acquired, which were symmetrically distributed about the lactate methyl resonance.

The off-resonance irradiation field strength (γB_2) applied to the tumor was estimated by measuring the flip angle in the region of interest generated by an RF pulse of a particular pulse duration. The off-resonance irradiation field strength value was taken as an average over the entire localized tumor volume.

In vivo T_1 and T_2 relaxation times are required for quantitative analysis of magnetization transfer as well as assessment of nonspecific RF bleedover. As noted previously (27), the sequence included an optional inversion pre-pulse for T_1 measurement and an optional spin-echo following the geMQC pulse for T_2 measurement. The observed T_1 and T_2 relaxation times for the methyl lactate protons were obtained in the absence of off-resonance irradiation and calculated using a five-point fit (TI varied from 1 msec to 5 sec) and a seven-point fit (TE varied from 156 msec to 464 msec), respectively; the number of excitations varied between 32 and 192, the sweep width was 2.5 kHz, N = 1 K points (complex), and the repetition time was 6 sec. Measurements were performed on a total of eight animals.

Each free induction decay (FID) was zero-filled to 4 K, and 6 Hz line broadening was applied prior to Fourier

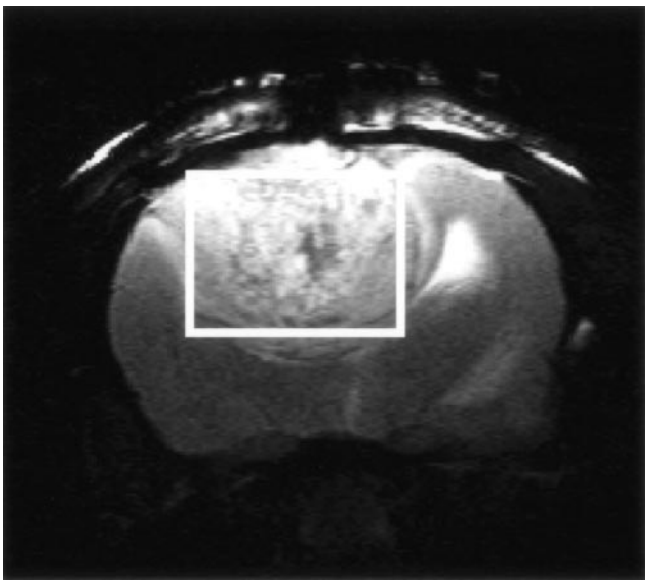

FIG. 1. T_2-weighted (TR/TE 1500/100 msec) scout image of a tumor-bearing rat brain. The frame delineates the representative volume from which the localized spectra were acquired.

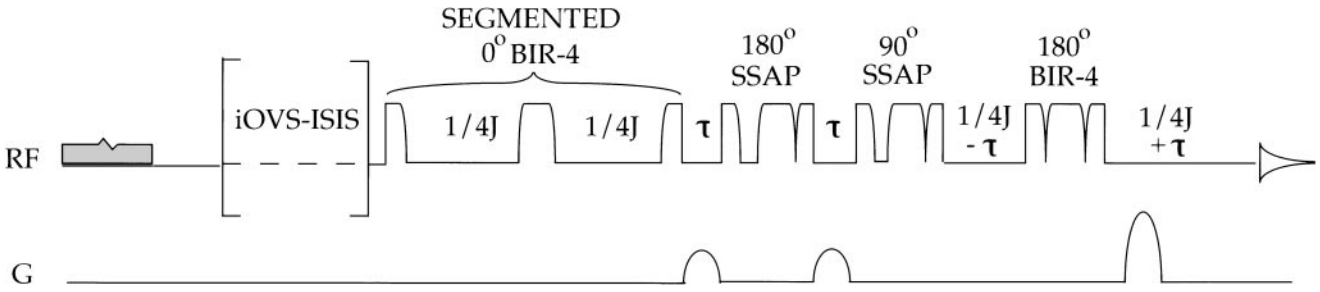

FIG. 2. Modified gradient-enhanced multiple quantum coherence (geMQC) editing sequence based on adiabatic RF pulses. Off-resonance RF irradiation was achieved with a long, low-amplitude RF pulse preceding the sequence (shaded area). iOVS-ISIS was used for single-voxel localization. For the determination of T_1 an optional inversion pulse preceded the editing portion of the sequence. Finally, an optional selective spin-echo (for refocusing the lactate resonance signal at 1.3 ppm) sequence followed the geMQC sequence for the measurement of T_2. The off-resonance irradiation was turned off during both relaxation time measurements.

transformation. After baseline correction, the lactate resonance amplitude of each spectrum was measured for the calculation of the intensity ratio, M_z^A/M_o^A, at different frequency offsets, but at constant B_2 field strength. M_o^A was determined from the spectrum acquired in the absence of off-resonance irradiation.

A computer program incorporating a simulated-annealing-steepest-descents optimization algorithm (28) was used to determine the relaxation and magnetization transfer-related parameters by fitting the steady-state solution of the Bloch equations incorporating magnetization into the experimental intensity ratio dispersion curves.

Deuterium MRS Experiments

^{2}H spectra and relaxation times were obtained at 46.07 MHz using a General Electric GN-300 spectrometer (currently serviced by Bruker, Billerica, MA) equipped with an Oxford Instruments (Oxford, UK) 7.05 T, wide-bore (89 mm) magnet. A GE 12 mm broad-band probe and 12 mm (o.d.) tubes (nonspinning) were used. Spin-lattice relaxation times (T_1) were measured using inversion recovery, whereas for T_2, the linewidth at half-height was used. (T_2 was assumed to be $\approx T_2^*$.) Phase cycling was used for all measurements. Chemical shifts were referenced to the natural abundance HDO resonance at 4.76 ppm (25°C). ^{2}H off-resonance rotating frame spin-lattice relaxation experiments using methodology previously described (24,29) were performed at 22°C. The spectral width used was 2000 Hz, and the B_2 power varied from 1.28 to 1.46 Gauss.

Blood was drawn from a healthy human adult volunteer. Sodium fluoride/potassium oxalate was used as an anticoagulant; red blood cells were removed by centrifugation to yield plasma. Sodium azide (0.02%) was added to prevent bacterial growth. Sodium DL-lactate-2,3,3,3-d_4 was purchased from MSD Isotopes (99.5 atom % D, MD-2273, lot 3484-0) and used for all experiments. Plasma sample L-lactate-d_4 concentrations were assayed using a kit manufactured by Sigma following instructions provided by the vendor (Procedure No. 826-UV). The assay results were doubled to account for the presumed presence of the D enantiomorph in the racemic DL-lactate-d_4 mixture.

Aliquots of stock DL-lactate-d_4 solution were added directly to 3.0 mL plasma samples yielding solutions of ca. 7, 14, 28, and 55 mM; the pH was adjusted to 7.8. Parallel samples of plasma without added lactate were prepared and treated in the same manner as the DL-lactate-d_4-containing samples to permit assay of endogenous lactate levels and total lactate.

MRS experiments involving the binding of DL-lactate-d_4 to bovine serum albumin and the proteins present in human plasma were performed as previously described (17,29).

Data Analysis

^{2}H off-resonance rotating frame spin-lattice relaxation experiment intensity ratio curves (R vs. ν_{off}) were analyzed as described previously (21,29,30) using nonlinear regression to obtain values for the ligand rotational correlation time and $R(\infty)$.

RESULTS

Rat Glioma MRS Studies

In all animals studied significant attenuation of the tumor lactate resonance signal intensity was observed when RF irradiation was applied within 30 kHz of the lactate methyl proton resonance at 1.3 ppm. The decrease in signal intensity was symmetrical about the resonance frequency and power dependent. Typically at 15–20% decrease in signal intensity was observed at a frequency offset of approximately 10 kHz and a preparation RF field strength of 0.08 Gauss ($\gamma B_2/2\pi$ = 350 Hz), as shown in Fig. 3. The spectrum with no observable lactate was obtained with the RF irradiation placed directly on the lactate methyl resonance, i.e., with zero frequency offset.

A representative in vivo methyl lactate intensity ratio dispersion curve [$R(=M_z/M_o)$ vs. ν_{off}] is shown in Fig. 4.

Off-resonance irradiation effects were observed to be the same within the signal-to-noise ratio of the experiment for 2 or 3 sec irradiation periods in two animals, suggesting that the measured lactate signal represented the steady state at the employed off-resonance field strength (e.g., 0.15 Gauss, $\gamma B_2/2\pi$ = 625 Hz) and offset frequency (10 kHz).

To assess quantitatively the effect of nonspecific off-resonance saturation (''bleedover'') the methyl resonance intensity of aqueous lactate in a spherical phantom was measured in the presence of off-resonance irradiation under identical experimental conditions. The result was

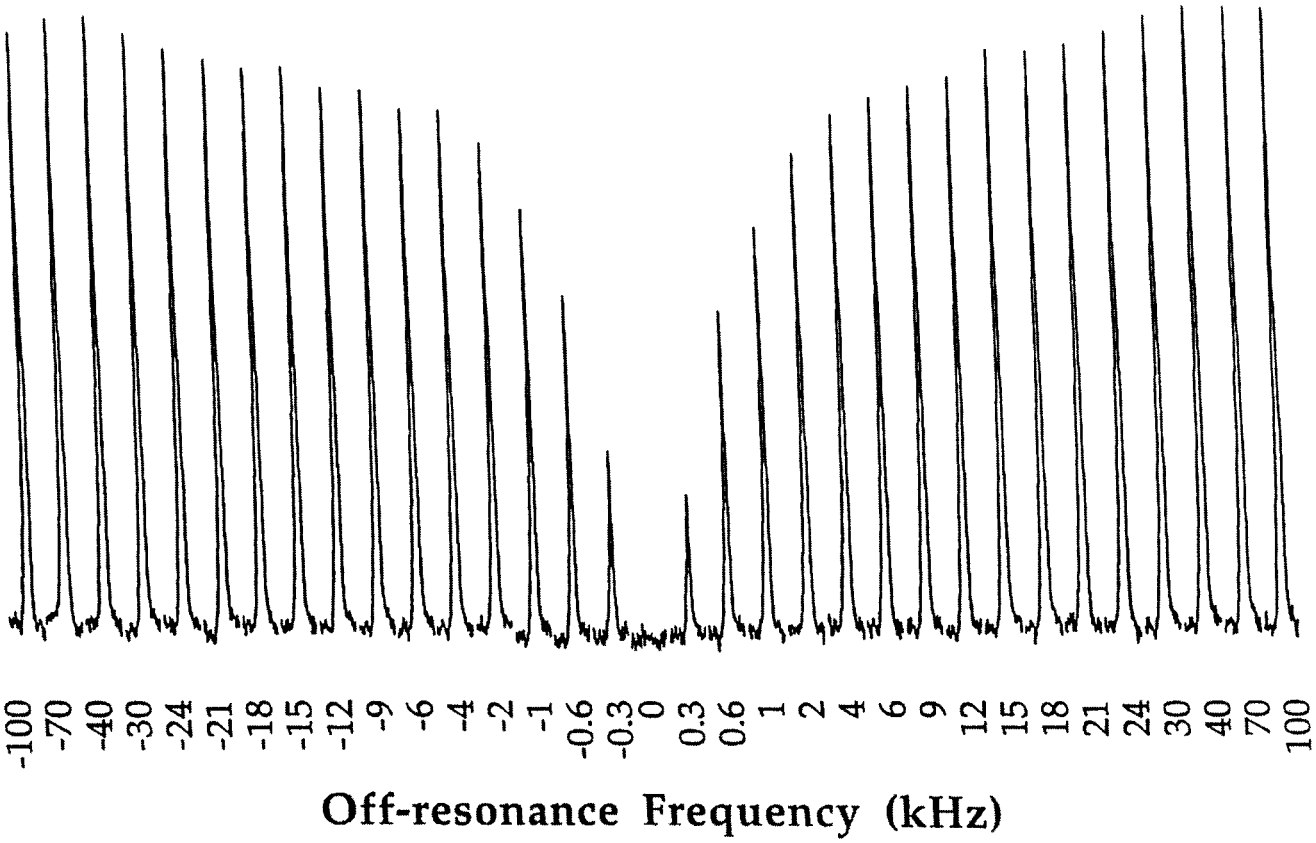

FIG. 3. ^{1}H MRS localized spectra displaying the lactate methyl resonance signal in rat C6 glioma acquired at different off-resonance irradiation frequencies. The localized volume was 230 mm^3. The off-resonance pulse duration was 3 sec, and the field strength, $\gamma B_2/2\pi$, was 347 Hz; TR/TE 6000/144 msec; NEX 32.

significantly different than found for the in vivo situation in that a decrease in the lactate resonance intensity was apparent only within an irradiation frequency offset of 4 kHz of the lactate resonance, as shown in Fig. 5. These results were in excellent agreement with numerical simulations of RF bleedover as depicted in this figure.

A two-compartment system consisting of a mobile proton spin pool with a Lorentzian line shape and a motionally restricted solid-like pool with a Gaussian line shape (16,18) was assumed to be applicable to rat brain lactate.

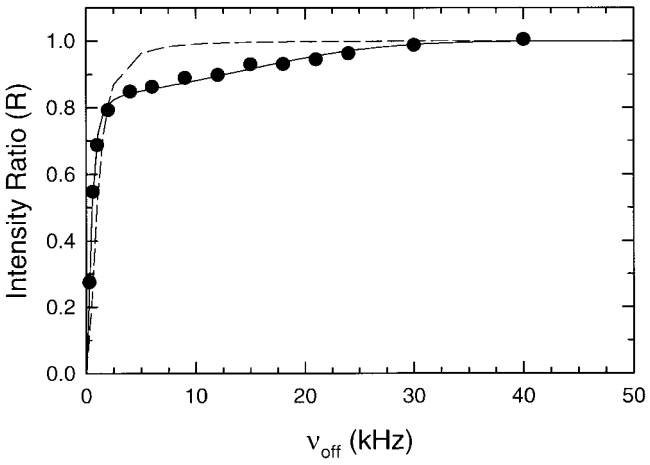

FIG. 4. Methyl lactate intensity ratio dispersion curve for rat C6 glioma (●). The solid line is the best fit curve to the experimental data using a binary spin bath model with the following parameters: R_T = 4.15 s^{-1}, f = 0.0014, and T_{2B} = 12.6 msec. The non-specific RF bleedover effect (- - - -) for the lactate methyl proton resonance was calculated using Eq. [3]. The B_2 off-resonance field strength was 0.07 Gauss.

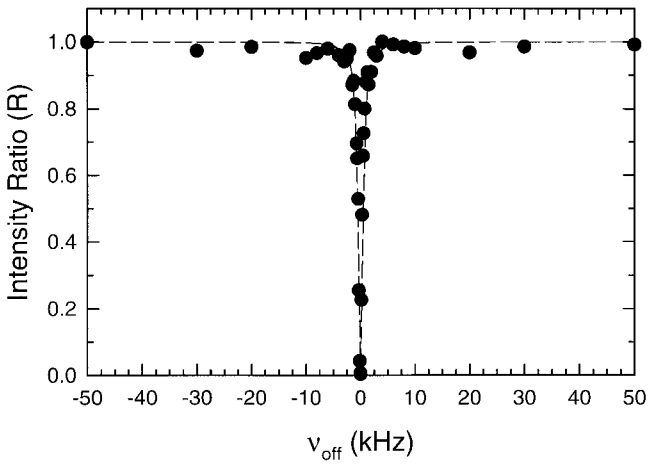

FIG. 5. Intensity ratio dispersion curve for aqueous lactate in a spherical phantom (●) and the theoretically calculated non-specific RF bleedover using Eq. [3] (- - - -). The B_2 off-resonance field strength was 0.07 Gauss. Experimentally determined T_1 and T_2 values of 1.43 sec and 554 msec were assumed.

Table 1
Observed Lactate Methyl Proton Relaxation Times for Rat Glioma Tumor Tissue

Animal no.	T_{1Aobs} (sec)	T_{2Aobs} (msec)	$\gamma B_{2A,B}/2\pi$ (Hz)
1	—	—	—
2	—	—	—
3	1.72	180	313
4	1.72	180	347
5	1.94	212	375
6	1.53	234	313
7	—	—	—
8	—	—	—
Mean ± SD	1.73 ± 0.17	202 ± 23	—

Values for T_1 and T_2 of the in vivo lactate methyl protons and the off-resonance irradiation field strength ($\gamma B_{2A,B}/2\pi$) are tabulated in Table 1. The symmetrical distribution of the resonance signal decrease due to off-resonance irradiation about the methyl lactate resonance implied that the lactate from the motionally restricted pool had the same resonance frequency as mobile pool lactate. Therefore, we assumed $\gamma B_{2A} = \gamma B_{2B}$ and $v_{off,A} = v_{off,B}$. A representative in vivo magnetization transfer data set showing the fitted curve superimposed on the corresponding experimental data as well as the theoretical RF bleedover curve is shown in Fig. 4. The best fit of the model (steady-state solution of the Bloch equations incorporating magnetization transfer) yielded unambiguous values for the following parameters: R_T, f, and T_{2B}, which are shown in Table 2 for each animal. Using these parameters and Eq. [2], the intrinsic T_2 (T_{2A} in Table 2) of the tumor lactate methyl proton was obtained. The fitted value for T_{1B} was less well defined, i.e., R_B could assume values within a large uncertainty range ($<400\ s^{-1}$) without causing significant change in the root-mean-square deviation (RMSD) (<0.001) of the fit. The values for T_{1A} listed in Table 2 are the values calculated using Eq. [1], whereas the values given for T_{1B} in Table 2 are based on the reasonable range of values characteristic of the T_1 of motionally restricted spins (31), i.e., the motionally restricted lactate pool. Comparison of the observed T_1 and T_2 values (tabulated in Table 1) with the intrinsic T_1 and T_2 values of the free pool (tabulated in Table 2) reveals that magnetization transfer does not significantly affect the tumor lactate spin-lattice relaxation time, whereas the transverse relaxation time was found to be considerably smaller than the observed value. Numerical values for magnetization transfer parameters obtained from all data sets acquired with different values of the off-resonance RF field strength yielded consistent results.

^{2}H Off-Resonance Rotating Frame Spin-Lattice Relaxation Model Lactate Studies

To explore the origin of the magnetization transfer effect manifested by lactate methyl protons and to provide a foundation for interpreting the in vivo results elaborated above, a series of ^{2}H off-resonance rotating frame spin-lattice relaxation studies were performed.

^{2}H spectra of deuterated lactate at different concentrations in human plasma at 22°C are shown in Fig. 6. For all samples, an average of 1.5 mM endogenous L-lactate was present, while the remainder was exogenously added DL-lactate-d_4. Plots of experimental ^{2}H spectral intensity ratio ($R = M_z/M_o$) of the CDOH and CD_3 deuterons for DL-lactate-d_4 plotted vs. frequency offset (v_{off}) corresponding to the concentrations above in human plasma are shown in Fig. 7. The solid line represents the best fit curve for the CDOH deuterons assuming isotropic tumbling. Values ranging from 4.6 to 5.9 nsec for $\tau_{o,eff}$ were obtained and are tabulated in Table 3. A value for $\tau_{o,eff}$ could not be obtained for the CD_3 resonance, indicating that the rotational correlation time was less than 1 nsec.

Table 3 tabulates the total lactate concentration, experimental RF field strength, and fitted $\tau_{o,eff}$ and experimental T_2 values for DL-lactate-d_4 in human plasma at 22°C. The value of $\tau_{o,eff}$ was found to be invariant at low lactate concentrations, indicating that $\tau_{o,eff}$ is approximately equal to $\tau_{o,B}$ under these conditions.

Analogous experiments were performed using BSA in place of plasma. The fitted $\tau_{o,eff}$ value for the DL-lactate-d_4 CDOH resonance in the presence of BSA was 3.5 ± 0.1 nsec, whereas the correlation time for the CD_3 DL-lactate-d_4 resonance was less than 1 nsec and could not be accurately determined.

The value for $\tau_{o,eff}$ of the CDOH resonance of lactate in the presence of BSA was found to be smaller than the rotational time of the protein, which was assumed to be 37 nsec (32). However, the fitted effective rotational correlation time is much longer than for the free species (ca. 0.01 nsec), indicating that the relaxation behavior of the motionally restricted species is what is observed. For this ligand, there appears to be a large degree of motion of the bound species relative to the reorientational motion of the protein. Furthermore, the CD_3 methyl group of DL-lactate-d_4

Table 2
Lactate Methyl Proton Magnetization Transfer Parameters and Intrinsic Relaxation Times for Rat Glioma Tumor Tissue*

Animal no.	R_T (s^{-1})	f	T_{1A} (sec)	T_{2A} (msec)	T_{1B} (sec)	T_{2B} (msec)
1	3.41	0.00067		647		10.5
2	4.03	0.00129		1086		12.4
3	4.15	0.00177		711		12.6
4	4.41	0.00143		873		12.6
5	2.91	0.00143		553		13.0
6	2.88	0.00161		718		14.5
7	3.21	0.0008		523		7.92
8	3.04	0.0013		523		7.92
Mean ± SD	3.5 ± 0.57	0.00121 ± 0.00051	1.73–1.74	710 ± 177	0.2–5.0	11.6 ± 2.0

*T_{1A} was determined using Eq. [1], whereas T_{1B} was based on assumed constraints (31).

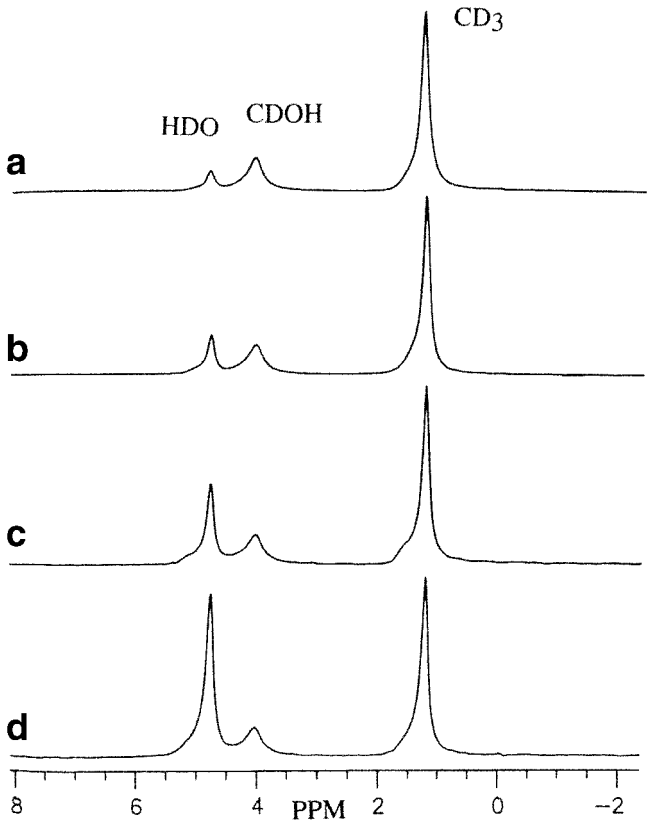

FIG. 6. ^{2}H MRS spectra of (**a**) 56.9 mM, (**b**) 29.1 mM, (**c**) 12.1 mM, and (**d**) 6.9 mM lactate in human plasma at 22°C. Approximately 1.5 mM endogenous L-lactate was present in each sample, whereas the balance was exogenously added DL-lactate-d_4. The spectra were referenced to HDO at 4.76 ppm.

possesses a relatively higher degree of motional freedom than the adjacent CDOH moiety.

The value for the T_2 relaxation time changed only by a factor of 1.3 when the lactate concentration was increased from 7 to 29 mM in the presence of human plasma. The T_2 relaxation times were in the range of 25 to 29 msec, which is compatible with the occurrence of small bound ligand fractions (29).

DISCUSSION

Three effects potentially contribute to resonance intensity attenuation by off-resonance irradiation of a nuclear spin system (16): a) off-resonance rotating frame spin-lattice relaxation effects arising from a single population of motionally restricted spins; b) nonspecific RF bleedover effects involving a single population of mobile spins; and c) magnetization (saturation) transfer between two or more spin populations representing mobile and motionally restricted components. These effects may act singly or in concert.

The experimentally observed relaxation time T_1/T_2 ratio of 8.6 for methyl lactate protons was significantly less than the theoretically calculated value (≈100) (using Eq. [3]) expected with significant off-resonance rotating frame spin-lattice relaxation contributions. Off-resonance rotating frame spin-lattice relaxation effects were therefore deemed to be insignificant. The dashed line in Fig. 4

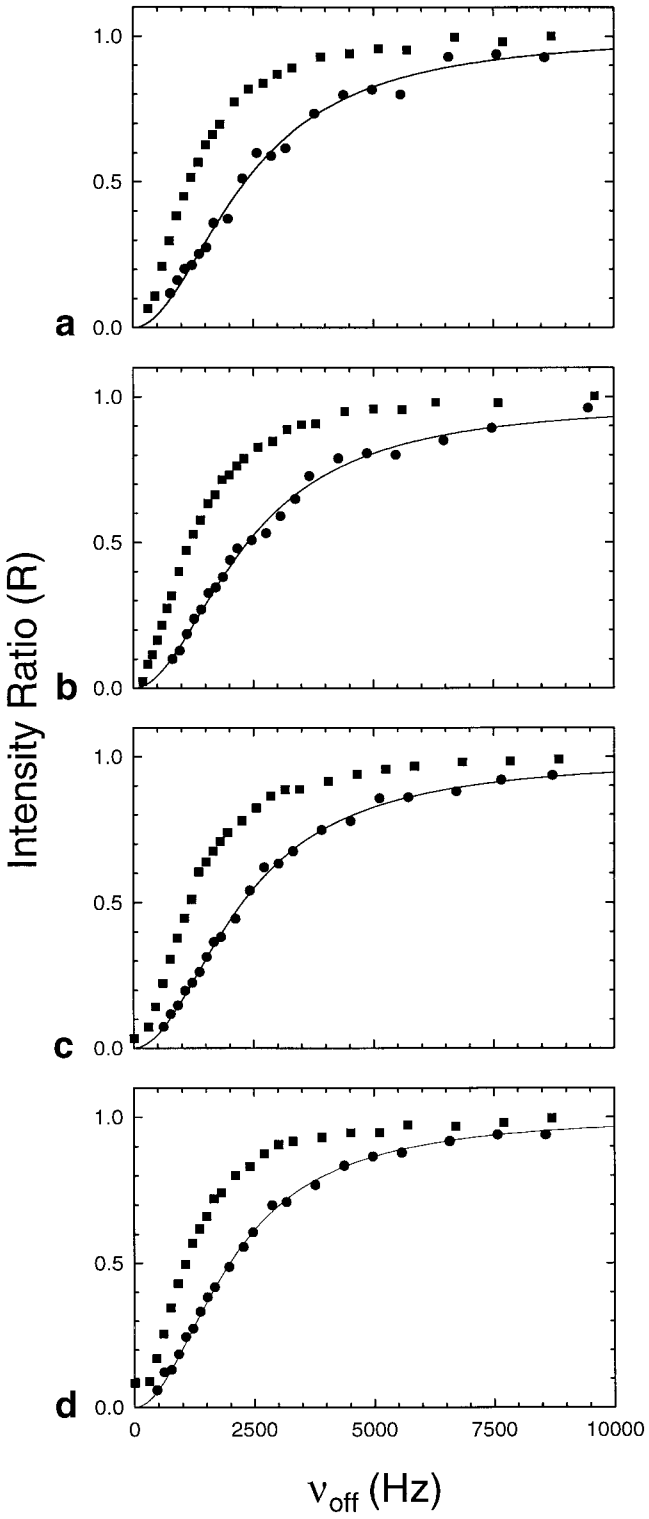

FIG. 7. Plots of the experimental ^{2}H spectral intensity ratio ($R = M_z/M_o$) vs. RF offset frequency (ν_{off}) for (**a**) 6.9 mM, (**b**) 12 mM, (**c**) 29 mM, and (**d**) 57 mM lactate in human plasma at 22°C. The CD_3 and CDOH resonances are denoted by (■) and (●), respectively. Total DL-lactate concentrations include both endogenous L-lactate (ca. 1.5 mM) and exogenously added DL-lactate-d_4. The solid line is the best fit curve assuming isotropic tumbling. Fitted $\tau_{o,eff}$ values for the CDOH resonance were (a) 5.9 ± 0.3 nsec, (b) 5.9 ± 0.2 nsec, (c) 5.5 ± 0.1 nsec, and (d) 4.6 ± 0.1 nsec. $\tau_{o,eff}$ for the CD_3 resonance was less than 1 nsec. The RF off-resonance field strengths were (a) 1.83, (b) 1.82, (c) 1.82, and (d) 1.77 Gauss.

Table 3
DL-Lactate Concentration, B_2 RF Field Strengths, Fitted $\tau_{o,eff}$, and Experimental T_2 Relaxation Times for the DL-Lactate-d_4 CDOH Resonance in Human Plasma at 22°C

[Lac][a] (mM)	B_2 (Gauss)	$\tau_{o,eff}$ (nsec)	T_2[b] (msec)
6.9	1.83	5.9 ± 0.3	25 ± 2
12	1.82	5.9 ± 0.2	26 ± 2
29	1.82	5.5 ± 0.1	28.7 ± 0.4
57	1.77	4.6 ± 0.1	31 ± 1

[a]Sum of endogenous L-lactate and exogenously added DL-lactate-d_4.
[b]Estimated from linewidth measurements ($T_2 \approx T_2^*$).

denotes the nonspecific RF bleedover effect calculated for the methyl lactate resonance using Eq. [3] as a function of RF irradiation frequency offset. The difference between this curve and the corresponding tissue data (Fig. 4) (maximum at a frequency offset of 10 kHz) implies that the observed resonance intensity attenuation produced by off-resonance irradiation of rat glioma in vivo arises from saturation transfer effects, thus demonstrating the occurrence of magnetization transfer between mobile and motionally restricted lactate methyl proton pools.

Analysis of experimental intensity ratio dispersion data provided unequivocal values for three of the four fitted parameters (Table 2). The derived lactate magnetization transfer parameters for rat glioma tissue, obtained assuming a two-component spin bath model, are comparable to those of other biological systems (22). The non-zero value obtained for R_T implies the occurrence of at least two lactate spin-pools in glioma tumor tissue coupled by magnetization transfer, which occurs by way of chemical exchange and/or dipolar coupling. The values for R_T and T_{2B} are consistent with the existence of a motionally restricted lactate pool characterized by fast transverse relaxation and magnetization transfer exchange with the observed lactate pool. By contrast, an equivocal value was determined for the spin-lattice relaxation rate of the motionally restricted lactate pool, R_B. The uncertainty in R_B is a consequence of the formalism used to obtain the magnetization transfer parameters. The term $(R_T/f + R_B)$, which appears in the steady-state solution of the Bloch equations incorporating magnetization transfer, represents the total ''flow'' of magnetization out of the motionally restricted spin pool as a consequence of magnetization transfer (R_T/f) and spin-lattice relaxation (R_B). For the situation where $R_T \gg f$ and $R_T/f \gg R_B$, the term $(R_T/f + R_B)$ is approximated by R_T/f; in turn, R_T/f is comparable to the second term in square brackets of the steady-state solution of the Bloch equations incorporating magnetization transfer, which is significantly larger than the product $R_B R_T$. Thus, the impact of variations in R_B on the intensity ratio M_z^A/M_o^A will be minimal and most likely not detectable within the experimental error of the measurements. We note that the uncertainty in the determination of R_B for an agar gel system (33) is likely to be due to similar considerations. In general, a two-component spin bath characterized by less or comparable exchange (R_T/f) relative to the intrinsic relaxation rate (R_B) allows precise assessment of spin-lattice relaxation of the motionally restricted spin pool by way of the magnetization transfer-based experiment.

A motionally restricted component is characterized by a relatively long T_1 (31). Thus, it is likely that R_B would assume a value between 0.2 and 5.0 s^{-1}. Hence, the intrinsic T_1 of the mobile spin pool, obtained using Eq. [1], would be approximately 1.73 sec assuming the experimentally determined values of R_A^{obs}, R_T, and f, with a marginal contribution from R_B.

The mole fraction of motionally restricted lactate determined in this study is small (<0.2%), suggesting that the contribution from this compartment is negligible in the quantification of lactate when the proton spectrum is acquired without nuclear spin perturbation of the motionally restricted pool by off-resonance RF irradiation. By contrast, Williams et al (13) reported that lactate concentration estimated from intact brain spectra was between 70 and 90% of the values obtained in vitro using extracts, whereas Kotitschke et al (11) reported that ca. 30% of the lactate present in rat brain cell cultures was not detected. Their quantitative MRS measurement protocol for lactate (at 11.75 T) included a 3 sec long presaturation RF pulse ($\nu_{off} \cong 1.8$ kHz) for water suppression. Neglecting the difference in the Larmor precessional frequencies employed in the two studies, our results obtained at 4.7 T indicated that low-power irradiation at $\nu_{off} \cong 1.8$ kHz could lead to a diminution in resonance intensity of ca. 20%. In another study (12) employing presaturation for water suppression, 25% of the lactate present in hypoxic or ischemic rat brain was observed by MRS at 5.6 T. Thus, the partial MRS visibility of lactate observed by Kotitschke et al (11) and others (12) may have arisen from magnetization transfer mediated by off-resonance irradiation. The occurrence of at least three pools of lactate, including tightly bound, in bacterial cells each with differing MRS visibility was demonstrated in bacterial cells (34). We conclude that the application of long-duration RF irradiation (e.g., presaturation, such as commonly employed for water suppression) can lead to partial or even complete saturation of a motionally restricted lactate pool (as well as other metabolites), resulting in a substantial decrease in resonance intensity by way of magnetization transfer effects. Such effects are accentuated by increasing off-resonance irradiation duration and/or field strength. Thus, when performing quantitative metabolite measurements using ^{1}H MRS spectra acquired with presaturation for water suppression, a significant underestimation of lactate may arise due to magnetization transfer-related signal loss.

Binding to macromolecular species has been suggested to account for the fraction of motionally restricted lactate (11). To explore directly the motional behavior of lactate in the presence of macromolecular species, rotational diffusion studies using off-resonance rotating frame spin-lattice relaxation were performed employing deuterated lactate in the presence of BSA and the human plasma proteins. Rydzewski and Schleich (24) recently showed that the off-resonance rotating frame spin-lattice relaxation experiment was applicable to the study of intermediate timescale molecular motions (correlation time range of ca. 2–500 nsec) of deuterium-labeled molecules. A subsequent study demonstrated that the ligand rotational diffusion data acquired in the presence of protein by means of the off-resonance rotating frame spin-lattice relaxation experiment reflected the approximate behavior of the ligand in

the bound state, provided that the fraction of bound ligand was at least 0.20 (17).

The isotropic tumbling associated with the lactate CDOH resonance is almost twice as fast as that calculated for TSP-d_4 in plasma (17), indicating either a larger amount of internal motion, an affinity for macromolecular species that tumble more rapidly, or a lack of strong interactions with the macromolecules present. This is especially true for the adjacent CD_3 moiety, which reorients at a rate outside the motional window of the off-resonance rotating frame spin lattice relaxation experiment, suggesting that hydrogen bonding plays a larger role than nonpolar bonding (hydrophobic interactions) in the binding interaction.

Two non-exchanging spin populations with different relaxation characteristics yield intensity ratio dispersion curves that exhibit biphasic behavior. Such behavior was not observed in this study, as shown in Fig. 7. Thus, a large portion of DL-lactate-d_4 at these concentrations is most likely to be in fast exchange between the mobile and motionally restricted state. Analysis of intensity ratio dispersion curves (R vs. v_{off}) for lactate in the presence of plasma proteins gave values for $\tau_{o,eff}$ of approximately 5–6 nsec, indicating motional restriction, possibly caused by the binding of lactate to macromolecular (protein) species. The derived value for $\tau_{o,eff}$ is somewhat smaller than that expected for tight binding to macromolecular species, which is most likely a consequence of ligand mobility in the bound state (17).

Previously reported proton MRS studies involving low concentrations of L-lactate (0.5–1.6 mM) in the presence of human plasma proteins indicated that lactate interacts with the high molecular weight fraction (>10 kDa), as manifested by the loss of lactate proton signal in spin-echo spectra (35,36). Furthermore, there appears to be two bound species, one with a weak association and one more tightly bound. Other studies suggest that the tightly bound lactate is associated with transferrin and α_1-antitrypsin, and not with immunoglobulins, albumin, or lipoproteins (35,36). Tumor lactate is primarily produced by glycolysis (37,38) and is exported by specific transporters (39–42). The binding of lactate to macromolecules in tumor tissue that have long rotational diffusion times, such as lactate dehydrogenase and monocarboxylate transporters, may contribute to the observed lactate methyl proton magnetization transfer.

Because the off-resonance rotating frame spin-lattice relaxation experiment senses the motional dynamics of primarily bound species, it has provided corroborating evidence for the association of lactate to macromolecular species, thereby possibly establishing a foundation to account for the observed magnetization transfer involving lactate protons in rat glioma tumor tissue. Macromolecular bound lactate in tissue would be expected to have considerably enhanced cross-relaxation, therefore accounting for the observed in vivo magnetization transfer of lactate in rat glioma tissue.

ACKNOWLEDGMENTS

This research was supported by National Institutes of Health grants EY-04033 (to T.S.) and CA-64338 and RR-08079 (to M.G.). We thank Dr. Douglas Brooks for help with the initial fits of magnetization transfer data, and Jim Loo and Dr. Hellmut Merkle for outstanding technical support.

REFERENCES

1. Luyten PR, Marien AJH, Heindel W, van Gerwen PHJ, Herholtz K, den Hollander JA, Friedmann G, Heiss W-D. Metabolic imaging of patients with intracranial tumors: H-1 MR spectroscopic imaging and PET. Radiology 1990;176:791–799.
2. Herholtz K, Heindel W, Luyten PR, den Hollander JA, Pietrzyk U, Voges J, Kugel H, Friedmann G, Weiss W-D. *In vivo* imaging of glucose consumption and lactate concentration in human gliomas. Ann Neurol 1992;31:319–327.
3. Ng TC, Xue M, Baqrnett G, Modic M. Grading of brain tumors using lactate and NAA/Cr acquired by high resolution proton chemical shift imaging. In: Proceedings of the SMR 2nd Annual Meeting, San Francisco, 1994. Vol. 1. p 126.
4. Bruhn H, Frahm J, Gyngell ML, Merboldt KD, Hanicke W, Sauter R, Hamburger C. Noninvasive differentiation of tumors with use of localized H-1 MR spectroscopy *in vivo:* initial experience with patients with cerebral tumors. Radiology 1989;172:541–548.
5. Schwickert G, Walente S, Sundfør K, Rofstad EK, Mueller-Klieser W. Correlation of high lactate levels in human cervical cancer with incidence of metastasis. Cancer Res 1995;55:4757–4759.
6. Sappy-Marinier D, Calabrese G, Hetherington HP, Fisher SNG, Deicken G, van Dyke C, Fein G, Weiner MW. Proton magnetic resonance spectroscopy of human brain: application to normal white matter, chronic infarction, and MRI white matter signal hyperintensities. Magn Reson Med 1992;26:313–327.
7. Berkelbach van der Sprenkel JW, Luyten PR, van Rijen PC, Tulleken CAF, den Hollander JA. Cerebral lactate detected by regional proton magnetic resonance spectroscopy in a patient with cerebral infarction. Stroke 1988;19:1556–1560.
8. Petroff OAC, Novotny EJ, Avison MJ, Rothman DL, Shulman RG, Pritchard PW. Cerebral lactate turnover after electroshock by proton observed carbon decoupled spectroscopy. In: Proceedings of the SMRM 8th Annual Meeting, Amsterdam, 1989. Vol. 1. p 332.
9. Schupp DG, Merkle H, Ellermann JM, Ke Y, Garwood M. Localized detection of glioma glycolysis using edited H-1 MRS. Magn Reson Med 1993;30:18–27.
10. Dreher W, Norris DG, Liebfritz D. Magnetization transfer affects the proton creatine/phosphocreatine signal intensity: in vivo demonstration in the rat brain. Magn. Reson. Med. 1994;31:81–84.
11. Kotitschke K, Schnackerz KD, Dringen R, Bogdahn U, Hasse A, von Kienlin M. Investigation of the H-1 NMR visibility of lactate in different rat and human brain cells. NMR in Biomed 1994;7:349–355.
12. Chang LH, Pereira BM, Weinstein PR, Keniry MA, Murphy-Boesch J, Litt L, James TL. Comparison of lactate concentration determinations in ischemic and hypoxic rat brains by *in vivo* and *in vitro* H-1 NMR spectroscopy. Magn Reson Med 1987;4:575–581.
13. Williams SR, Proctor E, Allen K, Gadian DG, Crockard HA. Quantitative estimation of lactate in the brain by H-1 NMR. Magn Reson Med 1988;7:425–431.
14. Wolff SD, Balaban RS. Magnetization transfer contrast (MTC) and tissue water proton relaxation *in vivo.* Magn Reson Med 1989;10:135–144.
15. Caines GH, Schleich T, Rydzewski JM. Incorporation of magnetization transfer into the formalism for rotating frame spin-lattice proton NMR relaxation in the presence of an off-resonance irradiation field. J Magn Reson 1991;95:558–566.
16. Schleich T, Caines GH, Rydzewski JM. Off-resonance rotating frame spin-lattice relaxation: theory, and *in vivo* MRS and MRI applications. In: Berliner L, Reuben J, editors. Biological magnetic resonance. Vol. 11. New York: Plenum Press; 1992. p 55–134.
17. Rydzewski JM, Schleich T. Deuterium off-resonance rotating frame spin-lattice relaxation of macromolecular bound ligands. Biophys J 1996;70:1472–1484.
18. Grad J, Bryant RG. Nuclear magnetic cross relaxation spectroscopy. J Magn Reson 1990;90:1–8.
19. O'Reilly DE, Poole Jr CP. Nuclear magnetic resonance of alumina containing transition metals. J Phys Chem 1963;67:1762–1771.
20. Luz Z, Meiboom S. Proton relaxation in dilute solutions of cobalt (II) and nickel (II) ions in methanol and the role of methanol exchange of the solvation sphere. J Chem Phys 1964;40:2686–2692.
21. Henkelman RM, Huang X, Xiang Q-S, Stanisz GJ, Swanson SD, Bronskill MJ. Quantitative interpretation of magnetization transfer. Magn Reson Med 1993;29:759–766.

22. Eng J, Ceckler TJ, Balaban RS. Quantitative H-1 magnetization transfer imaging *in vivo.* Magn Reson Med 1991;17:304–314.
23. Balaban RS, Ceckler TL. Magnetization transfer contrast in magnetic resonance imaging. Magn Reson Q 1992;8:116–137.
24. Rydzewski JM, Schleich T. Off-resonance rotating frame spin-lattice relaxation of quadrupolar (spin 1) nuclei. J Magn Reson 1994;105:129–136.
25. de Graaf RA, Luo Y, Terpstra M, Merkle H, Garwood M. A new localization method using an adiabatic pulse, BIR-4. J Magn Reson B 1995;106:245–252.
26. de Graaf RA, Luo Y, Terpstra M, Garwood M. Spectral editing with adiabatic pulses. J Magn Reson B 1995;109:184–193.
27. Terpstra M, High WB, Luo Y, de Graaf RA, Merkle H, Garwood M. Relationships among lactate concentration, blood flow, and histopathologic profiles in rat C6 glioma. NMR Biomed 1996;9:185–194.
28. Kuwata K, Brooks D, Yang H, Schleich T. Relaxation matrix formalism for rotating frame spin-lattice relaxation and magnetization transfer in the presence of an off-resonance irradiation field. J Magn Reson 1994;104:11–25.
29. Rydzewski JM. Application of ^{2}H and ^{13}C nuclear magnetic resonance spectroscopy to model and tissue systems. PhD Thesis, University of California, Santa Cruz, 1992.
30. Schleich T, Morgan CF, Caines GH. Determination of protein rotational correlation times by carbon-13 rotating frame spin-lattice relaxation in the presence of an off-resonance radiofrequency field. In: Vol. 176. Oppenheimer NJ, James TL, editors. Methods in enzymology. San Diego: Academic Press; 1989. p 55–134.
31. Harris RK. Nuclear magnetic resonance spectroscopy. A physiological view. New York: John Wiley & Sons; 1991.
32. Wang SX, Stevens A, Schleich T. Assessment of protein rotational diffusion by C-13 off-resonance rotating frame spin-lattice relaxation—effect of backbone and side-chain internal motion. Biopolymers 1993;33:1581–1589.
33. Tessier JJ, Dillon N, Carpenter AD, Hall LD. Interpretation of magnetization transfer and proton cross-relaxation spectra of biological tissues. J Magn Reson B 1994;107:138–144.
34. Hockings PD, Bendall MR, Rogers PJ. Selective intracellular lactate invisibility in *Enterococcus faecalis.* Magn Reson Med 1992;24:253–261.
35. Bell JD, Brown JCC, Kubal G, Sadler PJ. Nuclear magnetic resonance studies on blood plasma and plasma proteins: the recognition system for anions. Biochem Soc Trans 1988;16:714–715.
36. Bell JD, Brown JC, Kubal G, Sadler PJ. NMR invisible lactate in blood plasma. FEBS Lett 1988;235:81–86.
37. Warburg O. Lactic acid formation and growth. Biochem Zeitschr 1925;160:307.
38. Kallinowski F, Vaupel P, Runkel S, Berg G, Fortmeyer HP, Baessler KH, Wagner K. Glucose uptake, lactate release, ketone body turnover, metabolic micromilieu, and pH distributions in human breast cancer xenografts in nude rats. Cancer Res 1988;48:7264–7272.
39. Poole RC, Cranmer SL, Halestrap AP, Levi AJ. Substrate and inhibitor specificity of monocarboxylate transport into heart cells and erythrocytes. Further evidence for the existence of two distinct carriers. Biochem J 1990;269:827–829.
40. Poole RC, Halestrap AP, Price SJ, Levi AJ. The kinetics of transport of lactate and pyruvate into isolated cardiac myocytes from guinea pig. Kinetic evidence for the presence of carrier distinct from that in erythrocytes and hepatocytes. Biochem J 1989;264:409–418.
41. Spencer TL, Lehninger AL. L-lactate transport in Ehrlich ascites-tumor cells. Biochem J 1976;154:405–414.
42. Dubinsky WT, Racker E. The mechanism of lactate transport in human erythrocytes. J Membr Biol 1978;44:25–30.